

Multimodal imaging of a liver-on-a-chip model using labelled and label-free optical microscopy techniques

Supplementary section

Jan Majer^{1,2}, Aneesh Alex^{3,4}, Jindou Shi^{4,5,6}, Eric J. Chaney^{4,5}, Prabuddha Mukherjee^{4,5}, Darold R. Spillman Jr^{4,5,7}, Marina Marjanovic^{4,5,7,8}, Carla F. Newman¹, Reid M. Groseclose³, Peter D. Watson^{2,*}, Stephen A. Boppart^{4,5,6,7,8,9,*} and Steve R. Hood^{1,4,*}

¹Pre-Clinical Sciences, Research Technologies, GSK, Stevenage, UK

²School of Biosciences, Cardiff University, Cardiff, UK

³Pre-Clinical Sciences, Research Technologies, GSK, Collegeville, PA, USA

⁴GSK Center for Optical Molecular Imaging, University of Illinois Urbana-Champaign, Urbana, IL, USA

⁵Beckman Institute for Advanced Science and Technology, University of Illinois Urbana-Champaign, Urbana, IL, USA

⁶Department of Electrical and Computer Engineering, University of Illinois Urbana-Champaign, Urbana, IL, USA

⁷NIH/NIBIB P41 Center for Label-Free Imaging and Multiscale Biophotonics (CLIMB), University of Illinois Urbana-Champaign, Urbana, IL, USA

⁸Department of Bioengineering, University of Illinois Urbana-Champaign, Urbana, IL, USA

⁹Interdisciplinary Health Sciences Institute, University of Illinois Urbana-Champaign, Urbana, IL, USA

Comparison of ASO uptake in different pores of the liver-on-a-chip scaffold

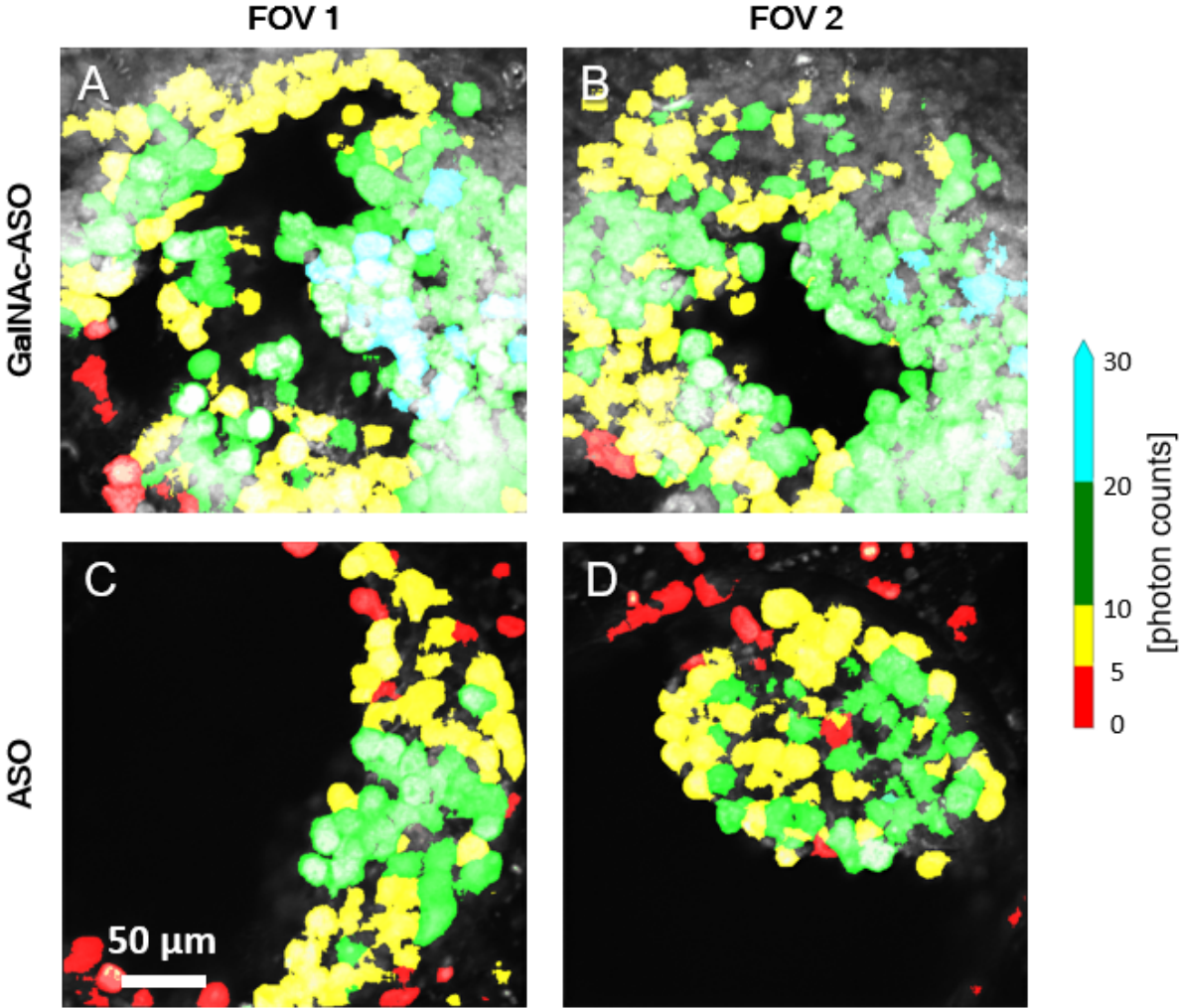


Figure S1: ASO uptake determined based on measured A488 fluorescence intensity from different pores of the scaffold that were treated with 2 μM GalNAc-ASO (A, B) and non-targeted ASO (C, D) at 1 h time point, respectively. FOV – field of view. Scale bar = 50 μm .

Cellular phenotypes in a liver-on-a-chip scaffold

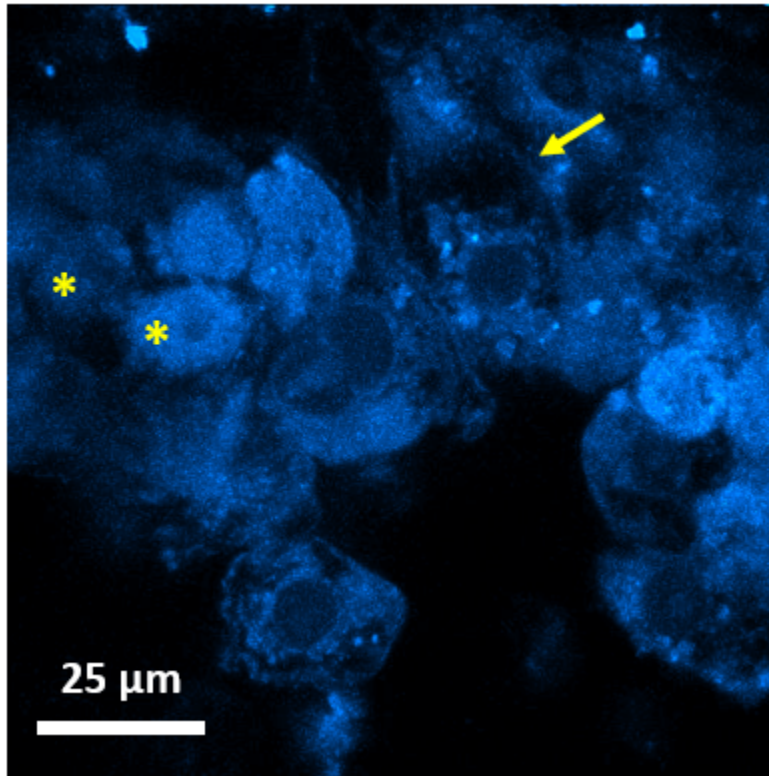


Figure S2: Cellular phenotypes observed in the liver-on-a-chip scaffold. Cells with circular and cuboidal morphologies were observed in the pores of a liver-on-a-chip scaffold. Cellular and sub-cellular morphological features were visible from the NAD(P)H autofluorescence signal, which was captured in the second detection channel of the custom-built multiphoton imaging system. Multiphoton images of microtissue formations obtained from a depth of 30 μm inside the pores of a vehicle control (PBS only) liver-on-a-chip scaffold obtained at 60x magnification. Arrow points toward the cuboidal hepatocyte and * denotes circular cells. Scale bar: 25 μm .

Manual segmentation of cuboidal hepatocytes and quantification of ASO uptake

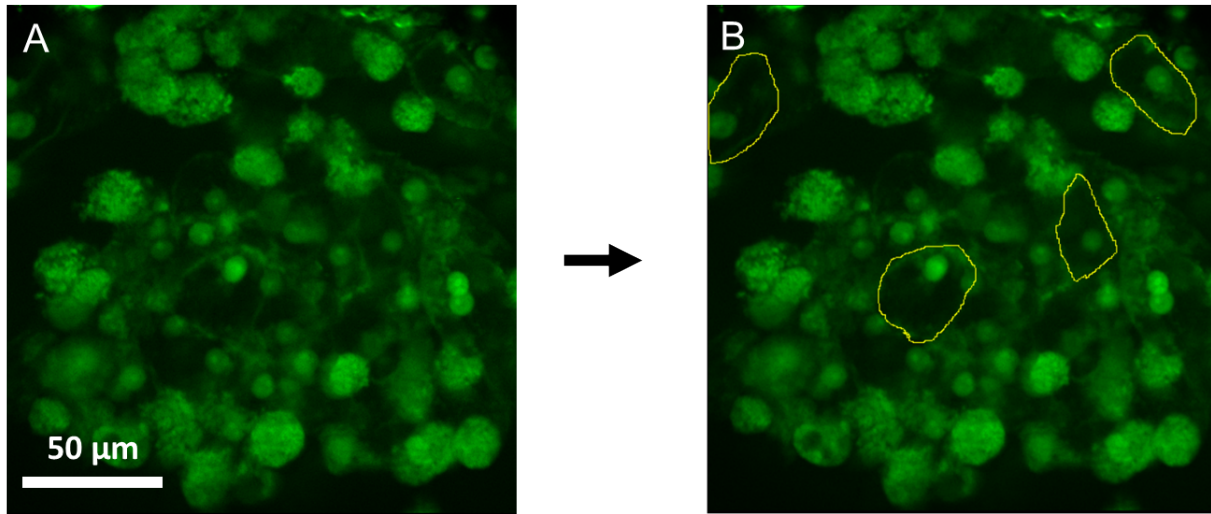


Figure S3: A representative image obtained from a liver-on-a-chip scaffold that was treated with A488-ASO-GalNAc 1 h post-treatment. A) Multiphoton image showing the fluorescence intensity detected in the A488 channel. B) Corresponding annotated image showing the manually segmented cuboidal hepatocytes. Scale bar = 50 μm.

Comparison of 1PF and 2PF penetration depth through nuclear A488 fluorescence signal

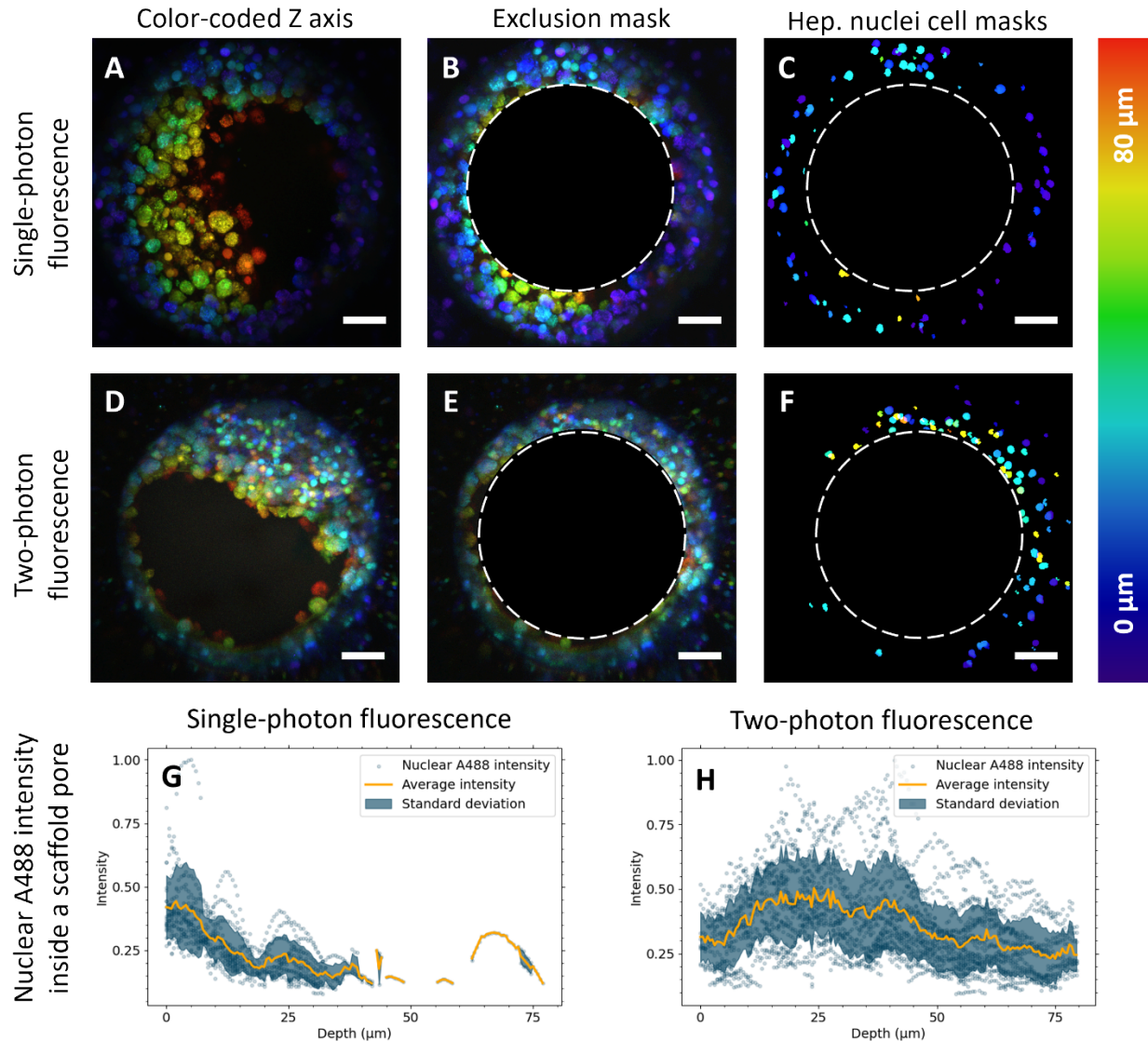


Figure S4: Cellpose algorithm and manual exclusion of the central pore region (to avoid new top layer cells appearing towards the pore center with the increased depth of focus) was used to generate masks quantification of signal loss with the sample depth. The depth information was transformed into a color-coded image using the Maximum intensity projection (Fiji ImageJ) along Z axis was used to flatten images for both A) 1PF and B) 2PF datasets. B, E) Pore center-excluding masks were manually created (dashed white circle). C, F) Nuclei masks were generated with a Nuclei model trained with >250 nuclei with 1PF and 2PF data, respectively. Scale bars = 50 μm . G, H) Masks were used to capture and average the fluorescence intensity of each nuclear object per Z plane (i.e., 1 dot = 1 nucleus per plane). The intensity scales are relative to the maximum intensity in each 3D dataset.

Light sheet microscopy

Precise sample positioning is crucial, especially in complex samples such as the liver-on-a-chip. The Zeiss Z.1 LSFM sample chamber facilitated accurate sample positioning, allowing for targeted illumination of scaffold pores by the light sheet and detection at a 90° angle relative to the sample. Rotating the sample along the vertical axis enabled collection of fluorescence emission from both sides of the scaffold pore excited from one of the two light sheet objective lenses.

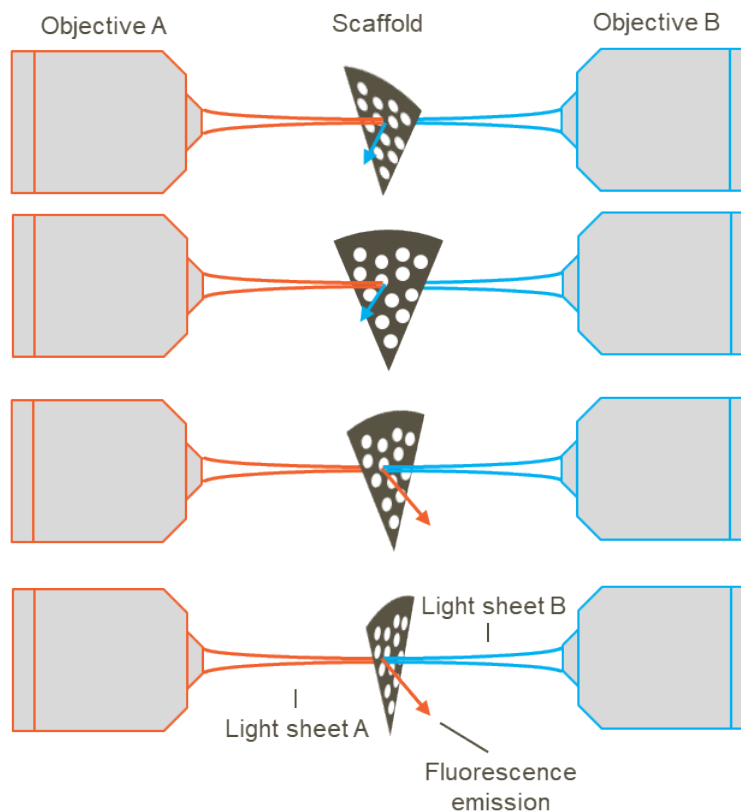


Figure S5: Sample orientation in LSFM.

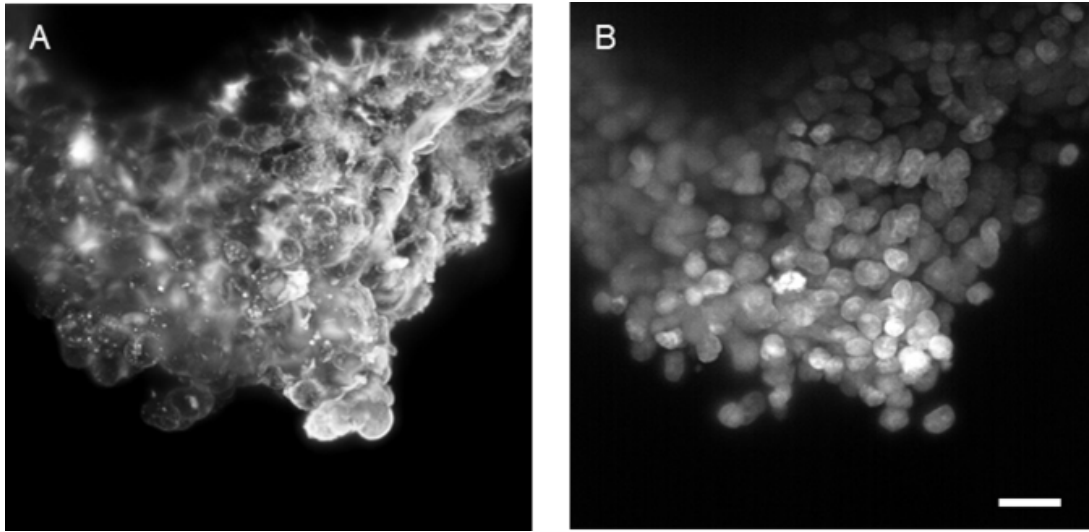


Figure S6: Validation of A) ConA and B) Hoechst PFA-fixed in untreated HepG2 spheroids. Scale bar = 20 μ m

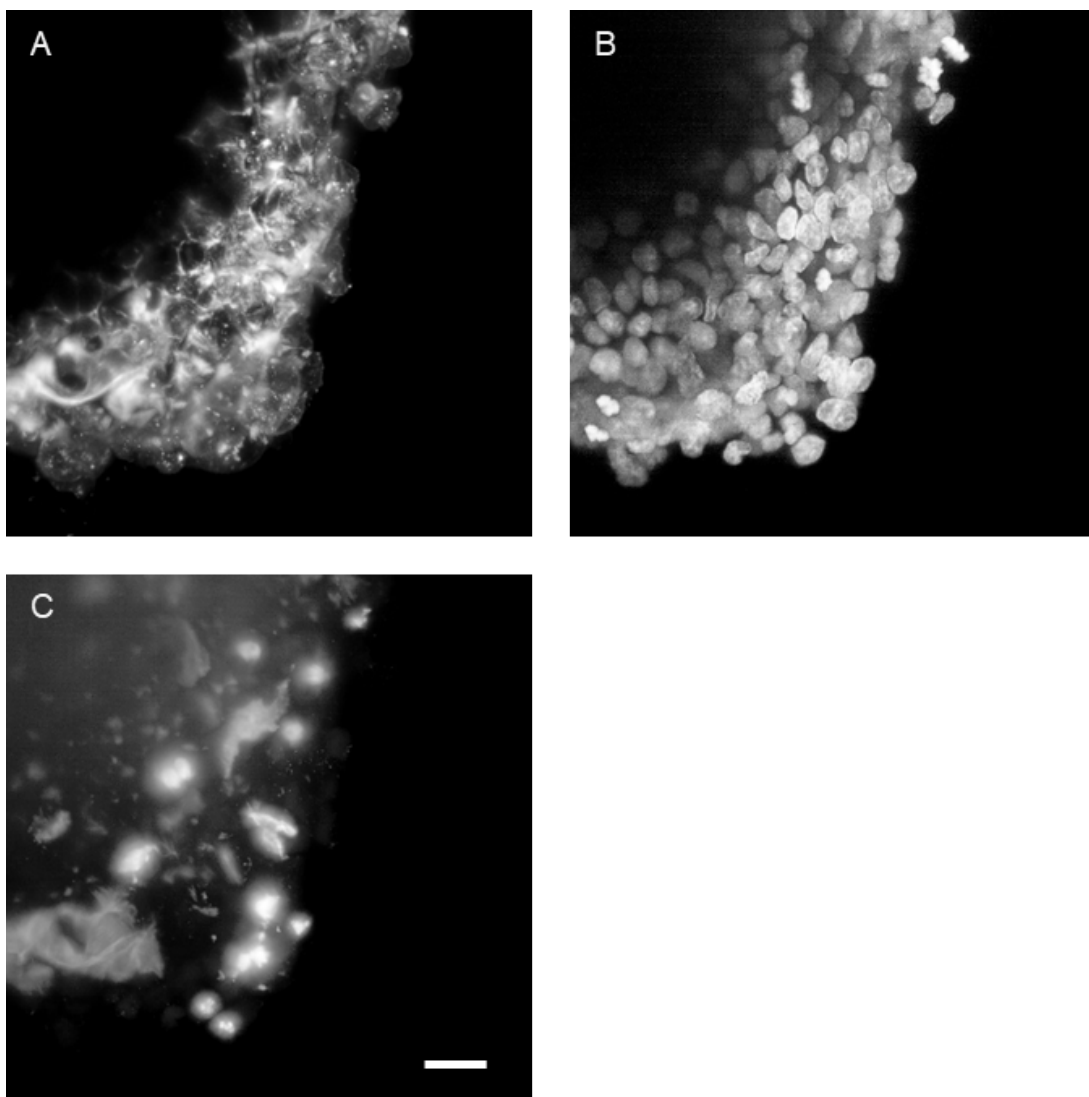


Figure S7: A) ConA and B) Hoechst, C) ASO distribution in A488-ASO-treated ($2\ \mu\text{M}$, 1 h) HepG2 spheroids. Staining was conducted after fixation. No permeabilization was done. Scale bar = $20\ \mu\text{m}$

Supplementary movies

ASO uptake (A488 fluorescence intensity) quantified in liver-on-a-chip scaffolds treated with PBS only (**Supplementary movie M1**), non-targeted ASO (**Supplementary movie M2**) and ASO-GalNAc (**Supplementary movie M3**), respectively. Cells detected in the pores under each of the treatment conditions were segmented along the depth of the pore (scaffold surface to 120 μm depth) using the Cellpose algorithm, and were color-coded based on the A488 fluorescence intensity measured in the corresponding channel. Corresponding color bar and scale bar are shown in Figs 3 and S1.